

Failure of Conductance Quantization in Two-Dimensional Topological Insulators due to Nonmagnetic Impurities

Pietro Novelli,^{1,2,*} Fabio Taddei,³ Andre K. Geim,⁴ and Marco Polini^{1,4}

¹*Istituto Italiano di Tecnologia, Graphene Labs, Via Morego 30, I-16163 Genova, Italy*

²*NEST, Scuola Normale Superiore, I-56126 Pisa, Italy*

³*NEST, Istituto Nanoscienze-CNR and Scuola Normale Superiore, I-56126 Pisa, Italy*

⁴*School of Physics and Astronomy, University of Manchester, Oxford Road, Manchester M13 9PL, United Kingdom*



(Received 16 July 2018; published 2 January 2019)

Despite topological protection and the absence of magnetic impurities, two-dimensional topological insulators display quantized conductance only in surprisingly short channels, which can be as short as 100 nm for atomically thin materials. We show that the combined action of short-range nonmagnetic impurities located near the edges and on site electron-electron interactions effectively creates noncollinear magnetic scatterers, and, hence, results in strong backscattering. The mechanism causes deviations from quantization even at zero temperature and for a modest strength of electron-electron interactions. Our theory provides a straightforward conceptual framework to explain experimental results, especially those in atomically thin crystals, plagued with short-range edge disorder.

DOI: 10.1103/PhysRevLett.122.016601

Introduction.—Research on spin-orbit coupling in graphene led Kane and Mele [1,2] to predict the existence of two-dimensional (2D) topological insulators (TIs). These are electron systems with a gap in the bulk density of states (DOS) and pairs of conducting edge states displaying helicity, i.e., spin-momentum locking. Because of Kramers theorem, in the absence of many-particle effects nonmagnetic impurities in a 2DTI cannot induce backscattering at a 2DTI edge, yielding conductance quantization against elastic disorder [3–8].

All experimental measurements on 2DTIs, however, show deviations from the expected quantized value of conductance $2e^2/h$, particularly in small-gap semiconductor heterostructures such as HgTe/CdHgTe and InAs/GaSb quantum wells [9–13], but also in atomically thin crystals such as WTe₂ [14,15]. On the other hand, the existence of conducting edge modes was clearly demonstrated via nonlocal measurements in Refs. [10–13]. Semiconducting heterostructures were extensively studied in the low-temperature regime (below 4 K) [9,13] because of their small energy gap. For channel lengths L shorter than $\sim 1 \mu\text{m}$, fluctuations of the conductance around the quantized value $2e^2/h$ were observed as a function of the back gate voltage. For longer channels, even the average conductance was found to deviate from $2e^2/h$ and even totally suppressed [16], when the edge was perturbed by a scanning tip. Among the 2DTIs realized by semiconducting heterostructures, the best results were obtained thanks to Si doping [13]. In these samples, conductance is quantized up to 1%–2% at very low temperatures. Monolayers of WTe₂ exhibit [14] conductance quantization up to 100 K, making them the 2DTIs existing

at the highest temperatures up to date, though displaying quantization only in short channels ($L \lesssim 100 \text{ nm}$).

The cause of the breakdown of conductance quantization is still poorly understood. Clearly, one possibility is the presence of an external magnetic field [9,14] or of magnetic impurities [17–19], which induce spin-flip scattering (thus backscattering). Magnetic impurities, however, are rare both in materials grown by molecular beam epitaxy [9–13] and in mechanically exfoliated crystals [14,15], but explain experimental data in the “extrinsic” case in which magnetic dopants are deliberately added to pristine three-dimensional TI samples [20,21]. Coupling between opposite edges, in very narrow samples or in purposely fabricated point contacts, can also induce backscattering [22–24], with no need of time-reversal symmetry breaking. Importantly, the breakdown of conductance quantization could arise from two-body interactions. In Ref. [3], it was suggested that electron-electron ($e-e$) interactions in 2DTIs can cause backscattering through a third-order perturbation-theory scattering process, whereas the spontaneous breaking of time-reversal symmetry due to interactions was studied in Ref. [25]. Interactions are also at the core of other mechanisms proposed to explain the spoiling of conductance quantization in 2DTIs. Backscattering resulting from weak $e-e$ interactions and an impurity potential, in the absence of axial spin symmetry, was considered in Ref. [26]. Deviations from $2e^2/h$ were found to scale like T^4 , at low temperatures T . The coupling of edge modes to charge puddles, naturally present in real samples, was accounted for in Refs. [27,28] and found to lead to a

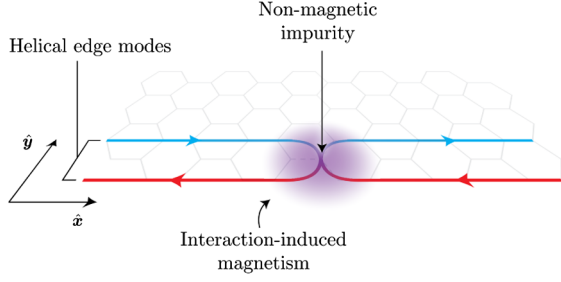


FIG. 1. A cartoon of the physical process introduced and analyzed in this Letter. At an edge of a 2DTI, a nonmagnetic short-range impurity can effectively act as a magnetic one due to its dressing via on site electron-electron interactions. The latter favor the formation of a local magnetic moment with non-zero in-plane components. These cause spin mixing and hence backscattering.

correction to the conductance scaling like T^4 at low temperatures. In contrast, recent experiments [14] show nearly temperature-independent conductance in 2DTIs. Another mechanism that leads to the breakdown of conductance quantization is related to the edge reconstruction [29], which can occur when the confining potential of the 2DTIs edges is not sufficiently sharp. Finally, the effects of Rashba spin-orbit coupling [30,31], phonons [32], nuclear spins [33,34], disordered probes [35], coupling to external baths [36], and noise [37] have also been analyzed.

In this Letter, we propose a simple mechanism, based on the interplay between nonmagnetic scatterers and e - e interactions, which leads to the breakdown of conductance quantization in 2DTIs, even at zero temperature, and can result in the total suppression of the conductance. Starting from the single-particle Kane-Mele Hamiltonian [1,2] describing a 2DTI ribbon, we consider the presence of short-range nonmagnetic impurities at its edges (see Fig. 1). As expected, this leads to an enhancement of the local DOS, as in the case of midgap states in graphene [38] and three-dimensional TIs [39–41]. In the presence of Hubbard-like e - e interactions, using the self-consistent unrestricted Hartree-Fock method, we show that these short-range defects favor the formation of local magnetic moments, leading to the spontaneous breakdown of time-reversal symmetry and backscattering.

Theoretical model.—We consider the Kane-Mele-Hubbard model [42,43],

$$\begin{aligned} \mathcal{H} = & t \sum_{\langle ij \rangle, \alpha} c_{i\alpha}^\dagger c_{j\alpha} + i\lambda \sum_{\langle\langle ij \rangle\rangle, \alpha, \beta} \nu_{ij} c_{i\alpha}^\dagger \sigma_{\alpha\beta}^z c_{j\beta} \\ & + U \sum_i c_{i\uparrow}^\dagger c_{i\uparrow} c_{i\downarrow}^\dagger c_{i\downarrow}. \end{aligned} \quad (1)$$

In Eq. (1), $c_{i\alpha}^\dagger$ ($c_{i\alpha}$) creates (destroys) an electron of spin α on the i -th site of a honeycomb lattice and σ^z is a 2×2 Pauli matrix acting on spin space. The sums over $\langle ij \rangle$ ($\langle\langle ij \rangle\rangle$) are intended between i and j being first (second) neighbors. The parameters t and λ are hopping energies between first

and second neighboring sites, respectively. The second term in Eq. (1) was introduced by Kane and Mele [1,2] as a time-reversal invariant version of the Haldane model [44] and is responsible for the existence of helical edge modes. The factor ν_{ij} is equal to ± 1 , with $\nu_{ji} = -\nu_{ij}$, depending on the orientation of the two nearest-neighbor bonds the electron traverses in going from site j to i : $\nu_{ij} = -1$ ($+1$) if the electron reaches the second neighbor going (anti-) clockwise. The last term accounts for local e - e repulsive interactions. Such a two-body term will be treated within mean-field theory. The key point here is that we are not interested in dealing accurately with strong correlations in 2DTIs [43]. Our aim is to utilize the simplest approach that enables us to capture an important effect stemming from local e - e interactions in the weak-coupling $U/t < 1$ regime. In this regime, mean-field theory is expected to be accurate and allows us to obtain an effective single-particle Hamiltonian, which can be used in combination with Landauer-Büttiker theory [45] to compute transport properties.

We consider a ribbon extending in the region $0 \leq x \leq L$, $0 \leq y \leq W$, with armchair edges and periodic boundary conditions in the \hat{x} -direction (see Fig. 1). In order to investigate the effect of atomic-scale defects, we assume the presence of one or two vacancies, which can be accounted for by dropping from the sums in Eq. (1) terms involving the lattice sites where the atoms are missing. The case of many vacancies can be tackled in a straightforward manner but lies beyond the scope of this Letter. Our main point, here, is to demonstrate the importance of local e - e interactions in dressing short-range nonmagnetic impurities in a magnetic fashion.

Using the usual Hartree-Fock decoupling [46], we can express Eq. (1) in the unrestricted Hartree-Fock approximation [47,48] as

$$\begin{aligned} \mathcal{H} \simeq & t \sum_{\langle ij \rangle, \alpha} c_{i\alpha}^\dagger c_{j\alpha} + i\lambda \sum_{\langle\langle ij \rangle\rangle, \alpha, \beta} \nu_{ij} c_{i\alpha}^\dagger \sigma_{\alpha\beta}^z c_{j\beta} \\ & + \frac{U}{2} \sum_{i, \alpha, \beta} c_{i\alpha}^\dagger (n_i \mathbb{1}_{\alpha\beta} - \mathbf{m}_i \cdot \boldsymbol{\sigma}_{\alpha\beta}) c_{i\beta} \\ & - \frac{U}{4} \sum_i (n_i^2 - |\mathbf{m}_i|^2), \end{aligned} \quad (2)$$

where $\mathbb{1}$ is the 2×2 identity matrix, $\boldsymbol{\sigma} = (\sigma^x, \sigma^y, \sigma^z)$ is a vector of 2×2 Pauli matrices acting on spin space, and we have defined the local mean electron density as

$$n_i = \left\langle \sum_{\alpha} c_{i\alpha}^\dagger c_{i\alpha} \right\rangle, \quad (3)$$

and the local mean spin polarization $\mathbf{s}_i = \hbar \mathbf{m}_i / 2 = \hbar (m_i^x, m_i^y, m_i^z) / 2$ with

$$\mathbf{m}_i = \left\langle \sum_{\alpha, \beta} c_{i\alpha}^\dagger \boldsymbol{\sigma}_{\alpha\beta} c_{i\beta} \right\rangle, \quad (4)$$

which must be determined self-consistently. In order to do so, we use an iterative algorithm [49] which involves the exact diagonalization of the Hamiltonian (2). Our calculations were performed at $T = 0$, but can easily be extended to finite temperature. Technicalities are reported in the Supplemental Material [50]. For $\lambda = 0$, i.e., when the second neighbor hopping term is neglected, the lattice is bipartite in the sense of Ref. [51] and Lieb theorem holds, so that a non-zero ground-state spin polarization rigorously follows from sublattice imbalance (i.e., different number of sites in the two sublattices). As we will see below, a ground-state spin polarization occurs even for $\lambda \neq 0$ —i.e., in the topological phase of Eq. (1) with gap $\delta_g = |6\sqrt{3}\lambda|$ [2]—where Lieb theorem does not apply. All numerical results below refer to a rectangular sample with $L = 45(\sqrt{3}/2)a$ and width $W = 25a$.

Ground-state spin polarization.—In Fig. 2, we plot the spatial profile of the three components— m_i^x , top panel, m_i^y , central panel, and m_i^z , bottom panel—of the dimensionless spin polarization (4), calculated at half filling for $\lambda/t = 0.09$ and $U/t = 0.1$, when a single vacancy is placed at $x = 23(\sqrt{3}/2)a$ and $y = a$, where a is the lattice parameter. The ground-state electron density n_i turns out to be nearly uniform.

The results show that spin polarization occurs around the vacancy, being vanishing elsewhere with the exception of asymmetric tails extending throughout the edge. This nicely agrees with the Stoner criterion, stating that a ground-state magnetization can occur in presence of a peak in the DOS. Indeed, a short-range defect generally hosts bound states localized around it, leading to an enhancement of the local DOS in proximity of the defect.

It is interesting to note that a finite spin polarization is bound to atomic-scale imperfections. Away from the vacancy the sample displays zero spin polarization. We thus expect that short-range edge roughness, which naturally occurs, e.g., in atomically thin crystals [14,15], as well can in general lead to interaction-induced spin polarization. We now move to analyze its effects on the transport properties of the system.

Breakdown of conductance quantization.—Because of spin-momentum locking, backscattering is induced by spin-flip events, which, in turn, are induced by the terms proportional to m_i^x and m_i^y in Eq. (2). Once the mean-field theory parameters n_i and \mathbf{m}_i are obtained, the conductance of the sample in a two-terminal setup (where one lead is attached to the left and the other to the right) can be calculated within the Landauer-Büttiker formalism [45]. In particular, at zero temperature, the differential conductance G is given by $G = (2e^2/h)\mathcal{T}$, \mathcal{T} being the transmission coefficient. Quantization of conductance is a consequence of \mathcal{T} being an integer number. We have calculated \mathcal{T} as a function of energy E for the mean-field Hamiltonian (2)—with n_i and \mathbf{m}_i calculated self-consistently—by utilizing

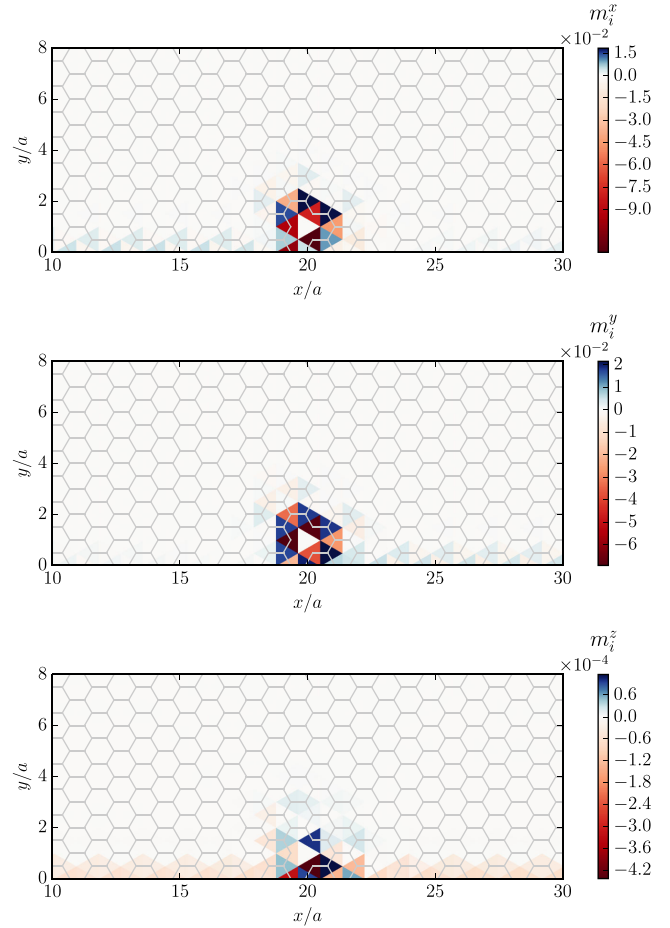


FIG. 2. Interaction-induced spin polarization near a vacancy. Color plot of the three components of the spatial profile of the dimensionless spin polarization \mathbf{m}_i around a vacancy located at $x = 23(\sqrt{3}/2)a$ and $y = a$. Top panel: m_i^x . Central panel: m_i^y . Bottom panel: m_i^z . From Eq. (2), it is clear that the components of \mathbf{m}_i lying on the $\hat{x} - \hat{y}$ plane are those leading to spin mixing and hence backscattering. Numerical results in this figure have been obtained by setting $\lambda/t = 0.09$ and $U/t = 0.1$.

the toolkit “KWANT” [52]. The leads are defined by the same Hamiltonian (2) with $\mathbf{m}_i = \mathbf{0}$ and n_i uniform and equal to 1 (corresponding to half filling) for every i .

Figures 3 and 4 show the transmission coefficient \mathcal{T} as a function of energy E ($E = 0$ denotes the energy at which the edge-mode dispersions cross in the leads) in the presence of one and two vacancies, respectively, and for different values of U/t . According to Fig. 3, relative to a single vacancy placed at $x = 23(\sqrt{3}/2)a$ and $y = a$, $\mathcal{T} < 2$ (thus conductance quantization is spoiled) for $E \approx 0$. In particular, pairs of sharp dips appear where backscattering is maximum and \mathcal{T} takes its minimum value, i.e., $\mathcal{T} \simeq 1$ due to the presence of an unperturbed propagating mode on the opposite edge of the sample. The main effect of increasing U from $0.1t$ to $0.5t$ is an enhancement of the separation between the dips, while the value of \mathcal{T} between the dips is slightly suppressed (by a few percent) with

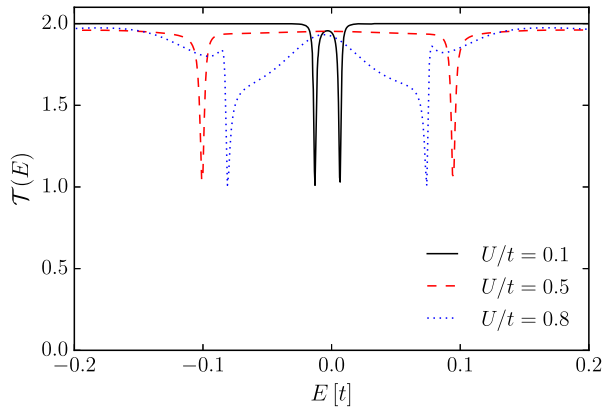


FIG. 3. Breakdown of conductance quantization for a single vacancy at the edge of a 2DTI. The transmission \mathcal{T} is plotted as a function of energy E (in units of t) at half filling and for energies lying in the gap δ_g . Different curves refer to different values of U/t . Numerical results in this figure have been obtained by setting $\lambda/t = 0.09$ ($\delta_g \simeq 0.93t$). Because on site e - e interactions produce a spin polarization with in-plane components near the vacancy, backscattering events occur at the same 2DTI edge and lead to the breakdown of conductance quantization, i.e., $\mathcal{T} < 2$.

respect to $\mathcal{T} = 2$, virtually independently of U . For larger values of U , for example at $U = 0.8t$, \mathcal{T} is much more affected presenting, apart from the pairs of dips, a sensible suppression in a larger range of energies. A few remarks are in order here. First, due to the approximate particle-hole symmetry of the model (1) at $\lambda/t \ll 1$, the transmission is a nearly perfectly even function of E . As already noted, the transmission is never below 1 because the unperturbed edge mode on the opposite side of the ribbon is perfectly conducting. Notice that at the energies where the dips occur the transmission relative to one edge mode nearly vanishes. Nearly total suppression of the conductance in a 2DTI was experimentally observed in Ref. [16]. Because the sample displays a finite spin polarization only around the impurity and the edge-mode wave functions decay exponentially away from the edge, the detrimental effects of a vacancy on G rapidly vanish as this is moved toward the center of the sample [50].

The behavior of \mathcal{T} for $U/t \ll 1$ can be understood by solving the problem of a magnetic δ -like impurity [53,54] at a single edge. In this regime, the dips in $\mathcal{T}(E)$ can be parametrized [50] by a Breit-Wigner dependence on E . Accordingly, such dips can be explained as antiresonances resulting from the localization of an electron around the impurity. Local DOS calculations [50] show that at the energy $E = \pm E_a$ of the dips the local DOS peaks around the impurity. This suggests that an electron with energy $E = \pm E_a$ traversing the sample gets localized in the bound state around the impurity and scattered back after a waiting time, which is inversely proportional to the width of the Breit-Wigner function.

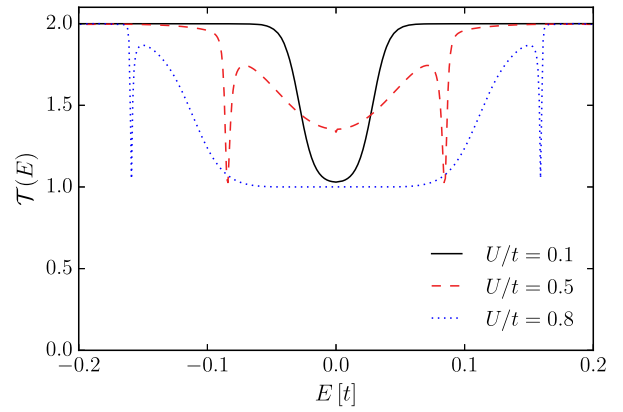


FIG. 4. Same as in Fig. 3 but for the case of two vacancies placed at $x = 23(\sqrt{3}/2)a$, $y = (3/2)a$ and $x = 26(\sqrt{3}/2)a$, $y = (1/2)a$.

Figure 4 shows the transmission calculated in the presence of two vacancies. We clearly see that \mathcal{T} is much more affected by the vacancies with respect to the case of a single vacancy, being suppressed in larger ranges of energy even in the weak-coupling regime. Moreover, for $U = 0.8t$ the transmission relative to one edge mode is suppressed to zero for $-0.1t < E < 0.1t$.

Summary and discussion.—We have shown that the combined action of short-range nonmagnetic impurities and on site e - e interactions in two-dimensional topological insulators leads to strong backscattering.

Strong deviations from quantization occur even in the zero-temperature limit. In contrast, all other theories [25–28] including e - e interactions yield deviations of the conductance from its quantized value, which vanish rapidly (i.e., like T^α with $\alpha \geq 4$) as a function of temperature T in the low-temperature limit. These deviations, scaling as power laws of T , arise because of scattering processes induced by e - e interactions. In the present Letter, on the other hand, we have shown that the ground state of the Kane-Mele-Hubbard model displays a $T = 0$ quantum phase transition from a paramagnetic to a magnetic state if short-range impurities and on site e - e interactions are taken into account. It is because of this ground-state quantum phase transition that our corrections to conductance quantization do not scale to zero in the $T \rightarrow 0$ limit. Ground-state edge reconstruction due to e - e interactions [29] also operates down to $T = 0$ but applies only to samples with smooth confining potentials. For example, for a Bernevig-Hughes-Zhang model applied to a HgTe/CdHgTe quantum well [4], edge reconstruction occurs [29] for confining potentials that decay slower than 13 meV/nm. Although certainly relevant for samples with smooth edges, the scenario of edge reconstruction is not expected to apply to atomically thin crystals [14,15], which possess sharp edges created either naturally by mechanical exfoliation or deliberately by etching.

In our theory, large deviations from quantization occur also in the weak-coupling $U/t < 1$ regime, where our

mean-field theory is expected to be accurate. In this case, the suppression of transmission as a function of energy can be interpreted in terms of antiresonances stemming from the time spent by an electron in the bound states formed near short-range impurities, before is backscattered due to spin-flipping terms in Eq. (2).

The formation of local magnetic moments in the presence of short-range impurities and on site e - e interactions is a general feature of bipartite lattices [38,51], for which the spectrum is particle-hole symmetric. Deep in the gap, any topological insulator possesses approximate particle-hole symmetry around the energy at which the edge modes cross. We have shown that small deviations from exact particle-hole symmetry (e.g., due to $\lambda \neq 0$ in our model) do not spoil the formation of local magnetic moments near short-range impurities. Furthermore, the same happens with the addition of Rashba spin-orbit coupling, which introduces extra terms breaking the exact particle-hole symmetry of (1) at $\lambda = 0$, as shown in the Supplemental Material [50]. We therefore expect that the spontaneous formation of local magnetic moments near short-range impurities induced by on site e - e interactions is a general feature of 2D topological insulators. In any event, recent Letter [55] has shown that a naturally occurring layered mineral (jacutingaite) realizes the Kane-Mele model.

We wish to thank M. I. Katsnelson and M. Gibertini for useful discussions. This work was supported by the Scuola Normale Superiore-Weizmann Institute of Science joint lab “QUANTRA” and the European Union’s Horizon 2020 research and innovation programme under Grant Agreement No. 785219—GrapheneCore2.

*pietro.novelli@sns.it

- [1] C. L. Kane and E. J. Mele, *Phys. Rev. Lett.* **95**, 226801 (2005).
- [2] C. L. Kane and E. J. Mele, *Phys. Rev. Lett.* **95**, 146802 (2005).
- [3] C. Xu and J. E. Moore, *Phys. Rev. B* **73**, 045322 (2006).
- [4] B. A. Bernevig, T. L. Hughes, and S.-C. Zhang, *Science* **314**, 1757 (2006).
- [5] M. Z. Hasan and C. L. Kane, *Rev. Mod. Phys.* **82**, 3045 (2010).
- [6] X.-L. Qi and S.-C. Zhang, *Rev. Mod. Phys.* **83**, 1057 (2011).
- [7] B. A. Bernevig and T. L. Hughes, *Topological Insulators and Topological Superconductors* (Princeton University Press, Princeton, NJ, 2013).
- [8] Y. Ren, Z. Qiao, and Q. Niu, *Rep. Prog. Phys.* **79**, 066501 (2016).
- [9] M. König, S. Wiedmann, C. Brüne, A. Roth, H. Buhmann, L. W. Molenkamp, X.-L. Qi, and S.-C. Zhang, *Science* **318**, 766 (2007).
- [10] A. Roth, C. Brüne, H. Buhmann, L. W. Molenkamp, J. Maciejko, X.-L. Qi, and S.-C. Zhang, *Science* **325**, 294 (2009).
- [11] K. Suzuki, Y. Harada, K. Onomitsu, and K. Muraki, *Phys. Rev. B* **87**, 235311 (2013).
- [12] G. Grabecki, J. Wróbel, M. Czapkiewicz, Ł. Cywiński, S. Gieraltowska, E. Guzewicz, M. Zholudev, V. Gavrilenko, N. N. Mikhailov, S. A. Dvoretzki, F. Teppe, W. Knap, and T. Dietl, *Phys. Rev. B* **88**, 165309 (2013).
- [13] L. Du, I. Knez, G. Sullivan, and R. R. Du, *Phys. Rev. Lett.* **114**, 096802 (2015).
- [14] S. Wu, V. Fatemi, Q. D. Gibson, K. Watanabe, T. Taniguchi, R. J. Cava, and P. Jarillo-Herrero, *Science* **359**, 76 (2018).
- [15] Y. Shi, J. Kahn, B. Niu, Z. Fei, B. Sun, X. Cai, B. A. Francisco, D. Wu, Z.-X. Shen, X. Xu, D. H. Cobden, and Y.-T. Cui, [arXiv:1807.09342](https://arxiv.org/abs/1807.09342).
- [16] M. König, M. Baenninger, A. G. F. Garcia, N. Harjee, B. L. Pruitt, C. Ames, P. Leubner, C. Brüne, H. Buhmann, L. W. Molenkamp, and D. Goldhaber-Gordon, *Phys. Rev. X* **3**, 021003 (2013).
- [17] Y. Tanaka, A. Furusaki, and K. A. Matveev, *Phys. Rev. Lett.* **106**, 236402 (2011).
- [18] J. Maciejko, C. Liu, Y. Oreg, X. L. Qi, C. Wu, and S.-C. Zhang, *Phys. Rev. Lett.* **102**, 256803 (2009).
- [19] B. L. Altshuler, I. L. Aleiner, and V. I. Yudson, *Phys. Rev. Lett.* **111**, 086401 (2013).
- [20] Y. L. Chen, J.-H. Chu, J. G. Analytis, Z. K. Liu, K. Igarashi, H.-H. Kuo, X. L. Qi, S. K. Mo, R. G. Moore, D. H. Lu, M. Hashimoto, T. Sasagawa, S.-C. Zhang, I. R. Fisher, Z. Hussain, and Z. X. Shen, *Science* **329**, 659 (2010).
- [21] L. A. Wray, S.-Y. Xu, Y. Xia, D. Hsieh, A. V. Fedorov, Y. S. Hor, R. J. Cava, A. Bansil, H. Lin, and M. Z. Hasan, *Nat. Phys.* **7**, 32 (2011).
- [22] A. Ström and H. Johannesson, *Phys. Rev. Lett.* **102**, 096806 (2009).
- [23] T. L. Schmidt, *Phys. Rev. Lett.* **107**, 096602 (2011).
- [24] C.-Y. Hou, E.-A. Kim, and C. Chamon, *Phys. Rev. Lett.* **102**, 076602 (2009).
- [25] C. Wu, B. A. Bernevig, and S.-C. Zhang, *Phys. Rev. Lett.* **96**, 106401 (2006).
- [26] T. L. Schmidt, S. Rachel, F. von Oppen, and L. I. Glazman, *Phys. Rev. Lett.* **108**, 156402 (2012).
- [27] J. I. Väyrynen, M. Goldstein, and L. I. Glazman, *Phys. Rev. Lett.* **110**, 216402 (2013).
- [28] J. I. Väyrynen, M. Goldstein, Y. Gefen, and L. I. Glazman, *Phys. Rev. B* **90**, 115309 (2014).
- [29] J. Wang, Y. Meir, and Y. Gefen, *Phys. Rev. Lett.* **118**, 046801 (2017).
- [30] A. Ström, H. Johannesson, and G. I. Japaridze, *Phys. Rev. Lett.* **104**, 256804 (2010).
- [31] F. Crépin, J. C. Budich, F. Dolcini, P. Recher, and B. Trauzettel, *Phys. Rev. B* **86**, 121106(R) (2012).
- [32] J. C. Budich, F. Dolcini, P. Recher, and B. Trauzettel, *Phys. Rev. Lett.* **108**, 086602 (2012).
- [33] C.-H. Hsu, P. Stano, J. Klinovaja, and D. Loss, *Phys. Rev. B* **96**, 081405 (2017).
- [34] C.-H. Hsu, P. Stano, J. Klinovaja, and D. Loss, *Phys. Rev. B* **97**, 125432 (2018).
- [35] A. Mani and C. Benjamin, *Phys. Rev. Applied* **6**, 014003 (2016).
- [36] A. A. Bagrov, F. Guinea, and M. I. Katsnelson, [arXiv:1805.11700](https://arxiv.org/abs/1805.11700).

- [37] J. I. Väyrynen, D. I. Pikulin, and J. Alicea, *Phys. Rev. Lett.* **121**, 106601 (2018).
- [38] M. I. Katsnelson, *Graphene: Carbon in Two Dimensions* (Cambridge University Press, Cambridge, England, 2012).
- [39] A. M. Black-Schaffer and A. V. Balatsky, *Phys. Rev. B* **85**, 121103 (2012).
- [40] A. M. Black-Schaffer and A. V. Balatsky, *Phys. Rev. B* **86**, 115433 (2012).
- [41] A. M. Black-Schaffer and D. Yudin, *Phys. Rev. B* **90**, 161413 (2014).
- [42] S. Rachel and K. Le Hur, *Phys. Rev. B* **82**, 075106 (2010).
- [43] S. Rachel, *Rep. Prog. Phys.* **81**, 116501 (2018).
- [44] F. D. M. Haldane, *Phys. Rev. Lett.* **61**, 2015 (1988).
- [45] S. Datta, *Electronic Transport in Mesoscopic Systems* (Cambridge University Press, Cambridge, England, 1995).
- [46] G. F. Giuliani and G. Vignale, *Quantum Theory of the Electron Liquid* (Cambridge University Press, Cambridge, England, 2005).
- [47] J. A. Vergés, E. Louis, P. S. Lomdahl, F. Guinea, and A. R. Bishop, *Phys. Rev. B* **43**, 6099 (1991).
- [48] J. A. Vergés, F. Guinea, and E. Louis, *Phys. Rev. B* **46**, 3562 (1992).
- [49] H. Feldner, Z. Y. Meng, A. Honecker, D. Cabra, S. Wessel, and F. F. Assaad, *Phys. Rev. B* **81**, 115416 (2010).
- [50] See Supplemental Material at <http://link.aps.org/supplemental/10.1103/PhysRevLett.122.016601> for technical details on the numerical procedures and further numerical results.
- [51] E. H. Lieb, *Phys. Rev. Lett.* **62**, 1201 (1989).
- [52] C. W. Groth, M. Wimmer, A. R. Akhmerov, and X. Waintal, *New J. Phys.* **16**, 063065 (2014).
- [53] X. Dang, J. D. Burton, and E. Y. Tsympal, *J. Phys. Condens. Matter* **28**, 38LT01 (2016).
- [54] J.-H. Zheng and M. A. Cazalilla, *Phys. Rev. B* **97**, 235402 (2018).
- [55] A. Marrazzo, M. Gibertini, D. Campi, N. Mounet, and N. Marzari, *Phys. Rev. Lett.* **120**, 117701 (2018).